PCCP

Accepted Manuscript

ROYAL SOCIETY OF CHEMISTRY

www.rsc.org/pccp

PCCP

PAPER

When ruthenia met titania: Achieving extraordinary catalytic activity at low temperature by nanostructuring oxides

Received 00th January 20xx,
Accepted 00th January 20xx

DOI: 10.1039/x0xx00000x

www.rsc.org/

J. Graciani,*[a] F. Yang,[b] J. Evans,[c] A. B. Vidal,[b,d] D. Stacchiola,[b] J. A. Rodriguez[b] and J. F. Sanz[a]

Nanostructured $RuO_x/TiO_2(110)$ catalysts have a remarkable catalytic activity for CO oxidation at temperatures in the range of 350-375 K. On the other hand a $RuO_2(110)$ surface has no activity. State-of-the-art DFT calculations indicate that the main reasons for such an impressive improving of the catalytic activity are: (i) a decrease of the diffusion barrier of adsorbed O atoms by around 40%, from 1.07 eV in $RuO_2(110)$ to 0.66 eV in $RuO_x/TiO_2(110)$, that explains the activity shift to lower temperatures, and (ii) a lowering of the barrier for the association of adsorbed CO and O species to give CO_2 (the main barrier for the CO oxidation reaction) by 20% passing from around 0.7 eV in $RuO_2(110)$ to 0.55 eV in $RuO_x/TiO_2(110)$. We show that the catalytic properties of ruthenia are strongly modified when supported as nanostructures on titania, attaining higher activity at temperatures 100 K lower than that needed with pure ruthenia. As in other systems consisting of ceria nanostructures supported on titania, nanostructured ruthenia shows strongly modified properties compared to the pure oxide, consolidating the nanostructuring of oxides as a main way to attain higher catalytic activity at lower temperatures.

Introduction

Removal of pollutants from the exhausts of automobiles is progressively but severely demanded by legislation around the world.[1,2,3] The so-called three-way catalysts used in the exhaust of automobiles try to eliminate at the same time NO_x species, hydrocarbons and CO, transforming them to N_2, H_2O and CO_2 respectively.[1,2,3,4] CO oxidation is usually taken as probe reaction for that purpose due to its simplicity and it has been one of the most widely studied heterogeneous catalytic reactions.[5] The oxidation of carbon monoxide is efficiently catalyzed by platinum group metal surfaces and related precious metals.[1,3,4,5] Generally they are supported as small metal particles on refractory oxide support as silica (SiO_2), alumina (Al_2O_3) and ceria (CeO_2), or refractory alumino-silicate materials like cordierite ($2MgO\cdot 2Al_2O_3\cdot 5SiO_2$).[3] It is generally accepted that CO and O_2 adsorb directly on the metal surface of Pt, Rh and Pd and then the reaction may take place.[6] However, the reaction mechanism in Ru is very different. Ru(0001) is a very poor catalyst for CO oxidation under UHV conditions.[7] High oxidizing conditions are required to form RuO_x species or RuO_2 that then exhibit high catalytic activity. Therefore, contrary to the other precious metals, the active phase in ruthenium catalyzed oxidations is the oxide..[7]

Ruthenia (RuO_2) is an excellent oxidation catalyst in heterogeneous catalysis at temperatures higher than 400 K, being 450 K the optimum temperature for CO oxidation. [8,9,10] The activity of ruthenia is even higher than that of Pt or Pd under excess O_2 at atmospheric pressure.[11] Although the availability of Ru is limited (about 20t/year) its lower price compared to the other precious metals (currently the Pt market price is 31.4 €/g, while the Ru price is 1.5 €/g)[12] makes it a good candidate for an eventual substitution of the usual Pt particles by RuO_2 particles in the exhaust catalysts in the automobile industry. Rh is even more expensive than Pt (31.75 €/g), and Pd is still 19.97 €/g (13 times more expensive than Ru).[12] Therefore, it seems interesting trying to design a ruthenia-based catalytic system with at least a similar catalytic activity than that of usual Pt-based catalysts.

Recently we have shown that RuO_2 grows on $TiO_2(110)$ forming nanowires that have special chemical properties.[13] A reversible $RuO_2 \leftrightarrow Ru$ transformation was observed when the temperature and background O_2 pressure were changed.[13] Figure 1 displays data for the oxidation of CO on $RuO_2/TiO_2(110)$ surfaces at 350 and 375 K. This is quite remarkable since at these temperatures $TiO_2(110)$ surfaces are not catalytically active,[13] while $RuO_2(110)$ surfaces has low activity,[8,13] achieving its highest activity at temperatures around 450K.[8] The change has to come from the nanostructured RuO_x species supported on $TiO_2(110)$. Analogous amazing catalytic effect has been observed for another nanostructured oxide supported on titanium dioxide: $CeO_x/TiO_2(110)$.[14,15,16] In that case the strong interaction with the support changed the electronic and geometrical structures of the supported CeO_x species, forcing them to form Ce_2O_3

[a] Departamento de Química Física. Universidad de Sevilla. 41012-Sevilla. SPAIN.
[b] Chemistry Department. Brookhaven National Laboratory. P.O. Box 5000. Upton, NY 11973-5000. USA.
[c] Facultad de Ciencias, Universidad Central de Venezuela, Caracas 1020-A. VENEZUELA.
[d] Centro de Química, Instituto Venezolano de Investigaciones Cientificas (IVIC), Apartado 21827, Caracas 1020-A, VENEZUELA.

dimers highly dispersed all over the surface. Obviously, the redox properties and catalytic activity of these strongly modified CeO_x species were completely different to those of CeO_2(111) surface.[17] The resulting system showed a tremendous catalytic activity for the water gas shift reaction, CO oxidation, and methanol synthesis from CO_2, when combined with metal nanoparticles.[14,15,16]

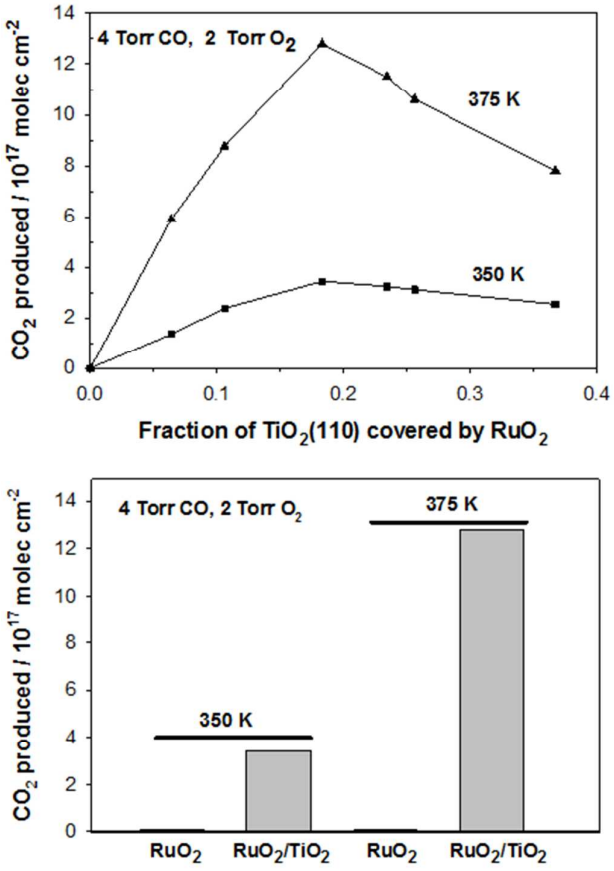

Fig. 1. Top: CO oxidation activity of RuO_2/TiO_2(110) as a function of RuO_2 coverage. The area of the titania substrate covered by RuO_2 was measured by ion scattering spectroscopy before carrying out the oxidation of CO. The reported values for the production of CO_2 were obtained after exposing the catalysts to 4 Torr of CO and 2 Torr of O_2 at 350 or 375 K for 5min. Bottom: comparison of the activity for CO oxidation of RuO_2(110) and a TiO_2(110) surface covered about 18% by RuO_2 nanowires. XPS showed only Ru^{4+} before and after CO oxidation.

Similar catalytic effects by nanostructuring oxides may be expected for supported RuO_x species. However, differently to the CeO_x/TiO_2(110) system, in the RuO_x/TiO_2(110) catalyst only structural optimizations and global energy trends have been calculated.[13] In our previous paper we characterized the system by means of STM, XPS and some DFT calculations, concluding that it consists of RuO_2 wires-like structure on TiO_2(110).[13] But why the system reaches that high activity at much lower temperature than pure ruthenia is still unexplained.

In contrast, the mechanism for CO oxidation on RuO_2(110) has been widely studied.[10] The chemical nature of the interaction of CO and O_2 with the ruthenia surface is well known and the main barriers for the reaction have been determined.[10] On the other hand, the reactivity of TiO_2(110) against CO and O_2 is negligible since the adsorption of CO is very weak (the strongest adsorbed CO molecules desorb above 170 K),[18] and O_2 molecule does not adsorb on the stoichiometric TiO_2(110) surface.[19] Therefore, if the RuO_x/TiO_2(110) catalyst is more active than RuO_2(110) surface the reason has to be in the modifications induced by the titania in the chemistry of the supported nanostructured ruthenia. In this work we compare the chemical behavior and the main CO oxidation reaction barriers of the RuO_x/TiO_2(110) system to those of the very well-known pure RuO_2(110) surface.

Computational methods

We model the RuO_2(110) surface with four O-Ru-O three-layers, keeping the two of the bottom fixed at the optimized bulk positions, allowing a vacuum region of 15 Å between repeated slabs. In order to avoid lateral interactions or effects coming from a high coverage, a (6x2) surface model was used. The nanostructured ruthenia on titania was modelled as follows: (a) TiO_2(110) surface consisted of four O-Ti-O three-layers, keeping the two of the bottom fixed at the optimized bulk positions, allowing a vacuum region of 15 Å between repeated slabs; (b) in order to achieve an isolated wire-like RuO_2(110) nanostructure a (6x3) surface model of the titania support was used; (c) a full-relaxed three atomic layer width (O-Ru-O) wire (6x1) was coupled to the titania support according to Ref. 13. The Perdew-Wang 91 (PW91) functional[20] was used for the exchange-correlation potential. The effect of the core electrons on the valence states was represented with the projector-augmented wave (PAW) approach[21], as implemented in the Vienna ab-initio simulation package, (VASP 5.3)[22,23], with the valence states defined for each atom as Ti (3s,3p,3d,4s), Ru(4s,4p,4d,5s), C(2s,2p), O(2s,2p), and H(1s) electrons, while the remaining electrons were kept frozen as core states. The valence electronic states are expanded in a basis of plane waves with a cutoff of 400 eV for the kinetic energy. In order to account for eventual reduction of the titania support (occupation of the Ti 3d states) a Hubbard-like U term was used, (GGA+U), according to the Dudarev *et al.* implementation,[24] which makes use of an effective parameter U_{eff}. We took a value U_{eff} =4.5 eV satisfactorily used in our previous works dealing with supported cerium oxide particles on titania[15,16,17,25]. Calculations were performed at the Γ point of the Brillouin zone. The transition states were found by the climbing nudged elastic band method (cNEB).

Experimental methods

Microscopy and Catalytic Tests. Clean TiO_2(110) surfaces were prepared by repeated cycles of argon-ion sputtering and annealing to 900K in presence of oxygen. Following previous

studies,[13] $Ru_3(CO)_{12}$ was used as a precursor for the deposition of ruthenium. $Ru_3(CO)_{12}$ vapor was introduced into the chamber by a doser, raising the chamber pressure to 1×10^{-8} Torr. While dosing the carbonyl, the TiO_2 crystal was held at 300 K with subsequent heating at elevated temperatures (600-700 K) in O_2 to induce the formation of RuO_x. This procedure does not leave C on the surface, since the final treatment involves oxidation under an O_2 background. The area of the titania surface covered by RuO_x was estimated using STM images and/or a combination of ISS and XPS. It is interesting to note that a different synthesis method based on depositing Ru from an electron beam evaporator lead to the formation of extended films of RuO_2 instead of nanostructured RuO_2 wires.[26] The microscopy studies were carried out in an Omicron variable temperature STM system. Chemically etched tungsten tips were used for imaging. Tests of catalytic activity for CO oxidation were conducted in a system which combines a batch reactor and a UHV chamber.[13,14,15,16] This UHV chamber (base pressure ca. 1 x 10^{-10} Torr) was equipped with instrumentation for X-ray photoelectron spectroscopy, low-energy electron diffraction, ion scattering spectroscopy, and temperature programmed desorption. Typically, the sample was transferred from the UHV chamber to the batch reactor at about 300 K without exposing to the air. The reactant gases were introduced (4 Torr of CO and 2 Torr of O_2), and then the sample was rapidly heated to the reaction temperature of 350 or 375 K. The amount of molecules produced was normalized by the active area exposed by the sample.

Results and discussion

First of all, we show the geometrical structure of the system as determined by STM experimental images and DFT calculations[13] and we compare new DFT-simulated STM images with the experimental ones (Figure 2). RuO_x species supported on TiO_2(110) are wire-like nanostructures epitaxially grown on the rutile structure showing the (110) surface. They coexist with some nanowires of TiO_x which exhibit a different height.[13] In the RuO_x nanowires, the well-known O bridging (O_{br}) row of the RuO_2(110) surface is in the middle on the wire and two rows of fivefold coordinated Ru atoms (traditionally so-called coordinatively unsaturated, *cus*, Ru_{cus})[10] are parallel at both sides of the O_{br} row (see Figure 2). In order to state clearly and coherently the nomenclature: we use the subscript "5c" to refer to fivefold coordinated metal atoms of the surface, either Ru_{5c} (traditionally Ru_{cus}) or Ti_{5c}; analogously, we will call "6c" to fully coordinated metal atoms (sixfold coordinated) either Ru_{6c} or Ti_{6c}; the undercoordinated oxygen atoms of the surface are called, as usual, bridging atoms with a subscript "br", O_{br}; finally, all remaining oxygen atoms are simply labelled as O.

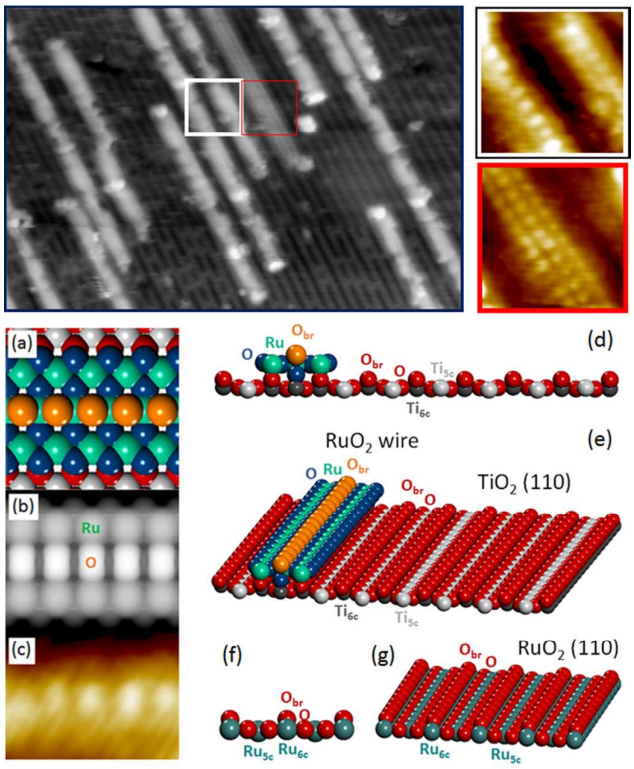

Fig. 2. Top: STM image for a small coverage of RuO_2 on TiO_2(110) (30 nm x 20 nm; V_t= 1.5 V; I_t= 1.2 nA). The insets on the right side magnify in the detail the structures of RuO_2 (white or black boxes) and TiO_x (red boxes). The original STM images were published before (Ref.13), we bring here those results for comparing more clearly to new DFT results. Bottom: Geometry of wire-like nanostructured RuO_2(110) supported on TiO_2(110) surface. (a) Top view of the atomic representation of the wire; (b) DFT-simulated STM image of the wire; (c) experimental STM image of the wire. (d) Side view of the RuO_2 wire supported on TiO_2(110), (e) 3D view of the same system, (f-g) side and 3D view of the RuO_2(110) surface. Colors: O atoms of pure RuO_2(110) and TiO_2(110) surfaces (red), O_{br} on top of the RuO_2 wire (orange), remaining O atoms of the wire (blue), Ti_{5c} (soft gray), Ti_{6c} (dark gray), Ru atoms in the wire (light green), Ru atoms in the RuO_2(110) surface (dark green). Only the outermost atoms of the system are represented for the sake of simplicity.

In the STM image of the supported wire, the brightest spots row in the middle corresponds to O_{br} atoms above the wire, while the other bright shadows at each side of the O_{br} row correspond to Ru_{5c} atoms of the wire. In the part of the STM image taken over the TiO_2(110)-support surface, the bright lines correspond, as usual, to the Ti_{5c} rows of the oxide surface.

CO oxidation catalyzed by this system was efficiently carried out at 350 or 375 K (Figure 1). According to the abundant literature, the active sites for the chemistry of the RuO_2(110) surface are the Ru_{5c} sites. At those sites, O_2 adsorbs and dissociates readily giving two O atoms adsorbed on top of two Ru_{5c} sites, and CO adsorbs strongly at the same position.[10] According to the ample bibliography, the factors that influence the catalytic activity of the RuO_2(110) surface are mainly three.[10] (1) the high diffusion energy barriers (higher than 1 eV) for both O and CO adsorbed species. Such barriers justify that only above 400 K, when adsorbed species are able to

diffuse, the catalytic activity starts to be high, reaching a maximum value at 450 K. (2) The main reaction energy barrier which corresponds to the association of the adsorbed O and CO species to give CO_2, being around 0.8-0.9 eV. (3) The stoichiometric ratio of reactants (O_2:2CO) since both are competing for the same reactive sites, namely Ru_{5c} (high pressures of O_2 saturates the surface avoiding the CO adsorption; high CO pressures not only saturates the surface against O_2 adsorption but also may reduce, even completely, the whole surface giving metallic Ru clusters at temperatures above 400K[27]). As we are using stoichiometric ratio of O_2 and CO, the higher activity of the TiO_2-supported nanostructured RuO_2 over the RuO_2(110) surface has to come from a lowering of either the diffusion barriers or the O-CO association barrier.

We have calculated these energy barriers on the RuO_2(110) surface and on TiO_2-supported wires-like RuO_2 nanostructures. The geometries and energies of the most significant transition states are represented in the Figure 3. The most important change is observed for the energy barrier of the diffusion of adsorbed O atoms along the Ru_{5c} rows. We obtained a value of 1.07 eV for the O-diffusion on RuO_2(110) that lowers to 0.66 eV in the wire-like RuO_2 supported nanostructures. This tremendous decrease (around 40%) of the diffusion barrier explains by itself the drop of the operating temperature from 450 K to 350 K. While adsorbed O atoms cannot diffuse on RuO_2(110) at 350 K they can do it readily on nanostructured RuO_2 supported on TiO_2(110). However, the diffusion barrier for adsorbed CO remains unchanged: 1.45 eV in RuO_2(110) and 1.44 eV in RuO_2/TiO_2(110). To have the CO oxidation reaction running we only need that one of both (O or CO) is able to move to reach the other and then react. Therefore, in the nanostructured RuO_2/TiO_2(110) system the motion of adsorbed O atoms makes the reaction able to start at lower temperatures.

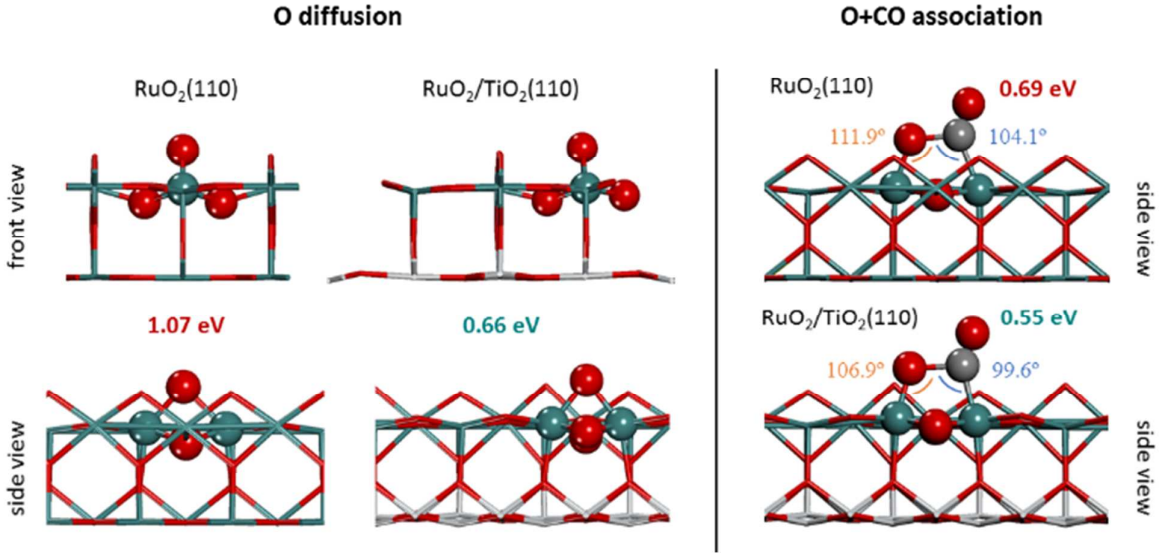

Fig. 3. Geometries and energies of the transition states corresponding to the diffusion of O atoms (left figures) and to the association of O and CO adsorbed species (right figures), for both RuO_2(110) surface and RuO_2/TiO_2(110) nanostructured oxide. Energy values: RuO_2(110) (red) and RuO_2/TiO_2(110) (green). Only the atoms directly implied in the transition state geometry are depicted as spheres, the others are shown as sticks. Colors: Oxygen (red), ruthenium (green), titanium (light gray) and carbon (dark gray). In the O+CO association transition states, the main angles are marked in orange and blue.

The reason of the decrease in the diffusion barrier for the adsorbed O atom is double. First, as it can be seen in the Figure 3, the motion of the adsorbed O atom from one Ru_{5c} to the other implies a large structural deformation of the O atoms around. They move inward repelled by the passing O anion. Obviously, this distortion is much easier to happen in a non-periodic structure (as the wire-like structure) than in a periodic 2D structure as pure RuO_2(110) or 1ML of extended RuO_2 on TiO_2(110), where the *x-y* relaxations are really hindered. Indeed, in our wire-like structure, one of the two O atoms that has to move inward (the outermost one) is free to do it since it is bonded only to two Ru_{5c} instead of three (see Figure 3). The second reason is that the distance Ru-Ru is shortened by around 5% in the 001 direction due to the epitaxial growing on TiO_2(110). That means that the Ru-O-Ru bridging transition state is easier to form. On the other hand, the unchanged CO diffusion barrier is due to the Blyholder bonding mechanism that takes place in the CO-RuO_2 bond.[10] This mechanism is tremendously directional: it is maximized in the direction perpendicular to the surface, being the CO molecule just on top of the Ru_{5c} atoms. It has been shown that Ru_{5c} atoms of the surface possess a "dangling bond" (eg^2sp^3) pointing outward the surface that contributes to the σ-donation part of the Blyholder mechanism while the π-back-donation involves mixed d_{xz}+d_{yz} Ru orbitals.[10] This mechanism is highly weakened when the CO molecule moves to bridging position between two Ru_{5c} in the transition state geometry. This Blyholder-bond break should happen equally in both RuO_2(110) and TiO_2-supported RuO_2 nanostructures, and that is why the diffusion barrier for CO remains unchanged.

Returning to Figure 3, we can see a significant decrease in the main reaction energy barrier: the O-CO association step. This barrier lowers from 0.69 eV in RuO_2(110) to 0.55 eV in RuO_2/TiO_2(110), which means a lowering of 20% in the association barrier. Therefore, not only the operating

temperature drops by around 100 K (due to the decrease of the O diffusion barrier by 40%) but also higher catalytic activity is expected because of the reduction of the association barrier by 20%. Again, the explanation of the decrease of the association barrier is mainly related to the shortened Ru-Ru distance in the 001 direction in the supported wire-like ruthenia nanostructures compared to pure ruthenia. Lesser structural deformation of the initial Ru_{5c}-O and Ru_{5c}-CO bonds is required to reach the transition state geometry on $RuO_2/TiO_2(110)$ than in $RuO_2(110)$ as O and CO adsorbed species are closer in the supported ruthenia. This effect can be easily seen comparing the angle values of the Ru_{5c}-C_{ads}-O_{ads} and Ru_{5c}-O_{ads}-C_{ads} bonds (where subscript *ads* stands for adsorbed) of the transition state geometry in both $RuO_2(110)$ and $RuO_2/TiO_2(110)$. Higher angles implies more strain of the Ru_{5c}-O and Ru_{5c}-CO initial bonds to form the transition state geometry (see Figure 3). The angle values for the Ru_{5c}-C_{ads}-O_{ads} bond were 104.1º and 99.6º for $RuO_2(110)$ and $RuO_2/TiO_2(110)$ respectively. Analogously for the Ru_{5c}-O_{ads}-C_{ads} bond we obtained angle values of 111.9º y 106.9º. First, we see a lesser strain in the geometry of the transition state in the titania-supported ruthenia than in pure ruthenia due to the shorter Ru-Ru distance. This explains the decrease in the association barrier on the nanostructured ruthenia. Second, we observe that the angle centered in the C atom is always smaller than the angle centered in the O atom. This is due to the different bonding mechanism. As the CO bonding mechanism is of the Blyholder type, slight deviations from 90º imply fast increase of the energy of the system, while the less orientation demanding O bond allows for a higher deformation at the same energy cost.

Conclusions

We have determined why nanostructured titania-supported ruthenia achieves higher catalytic activity for CO oxidation than pure ruthenia at much lower temperatures. Basically, the titania support imposes to supported ruthenia a epitaxial growth showing the (110) face and generating wire-like ruthenia nanostructures. This structurally modified ruthenia has a Ru-Ru distance shortened by 5% in the 001 direction, which propitiates a lower energy barrier for the formation of the O-CO transition state to give CO_2 (a decrease by 20%) and for the diffusion of adsorbed O atoms along that direction (a decrease around 40%). A larger lowering of the O-diffusion barrier arises from an additional stabilizing factor: the motion of the adsorbed O atoms implies a big structural deformation of the other nearby O atoms, and this structural distortion is much easier in a discrete nanostructure than in a pure perfect extended surface, in which the *x-y* relaxations are highly hindered. The huge decrease in the diffusion barrier makes possible to have the reaction working at 350 K, instead of the temperature of 450 K needed for the pure (110) ruthenia surface. The reduction of the O+CO association energy barrier by 20% enables also the nanostructured ruthenia to achieve higher catalytic activity than pure ruthenia. As in other systems studied before consisting of ceria nanostructures supported on titania,[14,15,16] nanostructured ruthenia on titania shows strongly modified properties compared to the pure oxide, consolidating the nanostructuring of oxides as a main way to attain new catalysts with higher activity at lower temperatures.

Acknowledgements

This work was funded by the Ministerio de Economía y Competitividad, Spain (grant MAT2012-31526), EU COST CM1104, and EU FEDER. Computational resources were provided by the Barcelona Supercomputing Center/Centro Nacional de Supercomputación (Spain). The research carried out at Brookhaven National Laboratory, was supported by the Division of Chemical Sciences, Geosciences, and Biosciences, Office of Basic Energy Sciences of the U.S. Department of Energy under contract DE-AC02-98CH10886. J.E. thanks INTEVEP and IDB for research grants that made possible part of this work at the Universidad Central de Venezuela.

References

1 H. S. Gandhi, G. W. Graham, R. W. McCabe, *J. Catal.,* 2003, **216**, 433.
2 M. Bowker, *Chem. Soc. Rev.* 2008, **37**, 2204.
3 H. Abe, *Science and technology trends – Quarterly review,* 2011, **39**, 21.
4 Y. Nishihata, J. Mizuki, T. Akao, H. Tanaka, M. Uenishi, M. Kimura, T. Okamoto, N. Hamada, *Nature,* 2002, **418**, 164.
5 A. W. Santra, D. W. Goodman, *Electrochim. Acta,* 2002, **47**, 3595.
6 T. Engel, G. Ertl, *The Chemical Physics of Solid Surfaces and Heterogeneous Catalysis*, Vol. 4; D. A. King, D. P. Woodruff, Eds.; Elsevier, Amsterdam, 1982.
7 Y. D. Kim, H. Over, G. Krabbes, G. Ertl, *Topics in Catal.,* 2001, **14**, 95.
8 R. Blume, M. Hävecker, S. Zafeiratos, D. Teschner, A. Knop-Gericke, R. Schögl, P. Dudin, A. Barinov, M. Kiskinova, *Catal. Today,* 2007, **124**, 71.
9 H. Over, Y. D. Kim, A. P. Seitsonen, S. Wendt, E. Lundgren, M. Schmid, P. Varga, A. Morgante, G. Ertl, *Science,* 2000, **287**, 1474.
10 H. Over, *Chem. Rev.,* 2012, **112**, 3356.
11 N. W. Cant, P. C. Hicks, B. S. Lennon, *J. Catal.,* 1978, **54**, 372.
12 http://www.infomine.com/investment/metal-prices/ (November 7th 2014).

13 F. Yang, S. Kundu, A. B. Vidal, J. Graciani, P. J. Ramirez, S. D. Senanayake, D. Stacchiola, J. Evans, P. Liu, J. F. Sanz, et al. *Angew. Chem. Int. Ed.,* 2011, **50**, 10198.

14 J. Graciani, K. Mudiyanselage, F. Xu, A. E. Baber, J. Evans, S. D. Senanayake, D. J. Stacchiola, P. Liu, J. Hrbek, J.F. Sanz, et al. *Science,* 2014, **345**, 546.

15 J. B. Park, J. Graciani, J. Evans, D. Stacchiola, S. Ma, P. Liu, A. Nambu, J. F. Sanz, J. Hrbek, J. A. Rodriguez, *Proc. Natl. Acad. Sciences (USA),* 2009, **106**, 4975.

16 J. B. Park, J. Graciani, J. Evans, D. Stacchiola, S. D. Senanayake, L. Barrio, P. Liu, J. F. Sanz, J. Hrbek, J. A. Rodriguez, *J. Am. Chem. Soc.,* 2010, **132**, 356.

17 J. Graciani, J.J. Plata, J.F. Sanz, P. Liu, J.A. Rodriguez, *J. Chem. Phys.,* 2010, **132**, 104703.

18 C. L. Pang, R. Lindsay, G. Thornton, *Chem. Rev.,* 2013, **113**, 3887.

19 C. L. Pang, R. Lindsay, G. Thornton, *Chem. Soc. Rev.,* 2008, **37**, 2328.

20 J. Perdew, Y. Wang, *Phys. Rev. B,* 1992, **45**, 13244.

21 G. Kresse, J. Joubert, *Phys. Rev. B,* 1999, **59**, 1758.

22 G. Kresse, J. Hafner, *Phys. Rev. B,* 1993, **47**, 558.

23 G. Kresse, J. Furthmuller, *Comput. Mater. Sci.,* 1996, **6**, 15.

24 S. L. Dudarev, G. A. Botton, S. Y. Savrasov, C. J. Humphreys, A. P. Sutton, *Phys. Rev. B,* 1998, **57**, 1505.

25 A. C. Johnston-Peck, S. D. Senanayake, J. J. Plata, S. Kundu, W. Xu, L. Barrio, J. Graciani, J. F. Sanz, R. M. Navarro, J. L. Fierro, et al. *J. Phys. Chem. C,* 2013, **117**, 14463.

26 Y. He, D. Langsdorf, L. Li, H. Over, *J. Phys. Chem. C,* 2015, **119**, 2692.

27 Y. B. He, M. Knapp, E. Lundgren, H. Over, *J. Phys. Chem. B,* 2005, **109**, 21825.